First ICRF Heating Experiment in the Large Helical Device

T. Mutoh, R. Kumazawa, T. Seki, K. Saito[1], F. Shimpo, G. Nomura, T. Watari, X. Jikang[2], G. Cattanei[3], H. Okada[4], K. Ohkubo, M. Sato, S. Kubo, T. Shimozuma, H. Idei, Y. Yoshimura, O. Kaneko, Y. Takeiri, M. Osakabe, Y. Oka, K. Tsumori, A. Komori, H. Yamada, K. Watanabe, S. Sakakibara, M. Shoji, R. Sakamoto, S. Inagaki, J. Miyazawa, S. Morita, K. Tanaka, B. J. Peterson, S. Murakami, T. Minami, S. Ohdachi, S. Kado, K. Narihara, H. Sasao, H. Suzuki, K. Kawahata, N. Ohyabu, Y. Nakamura, H. Funaba, S. Masuzaki, S. Muto, K. Sato, T. Morisaki, S. Sudo, Y. Nagayama, T. Watanabe, M. Sasao, K. Ida, N. Noda, K. Yamazaki, K. Akaishi, A. Sagara, K. Nishimura, T. Ozaki, K. Toi, O. Motojima, M. Fujiwara, A. Iiyoshi, LHD Exp.Group1 and 2

National Institute for Fusion Science, 322-6 Oroshi-cho, Toki, 509-5292 Japan
[1] Faculty of Engineering, Nagoya University, Furo-cho, Nagoya, Japan
[2] Institute of Plasma Physics, Academia Sinica, 230031, Hefei, Anhui, China
[3] Max-planck-Institut fuer Plasmaphysik, Euratom Association,D-85748,Garching,Germany
[4] Institute of Advanced Energy, Kyoto University, Gokasho, Uji, Kyoto, Japan

INTRODUCTION

First ICRF heating experiment in the Large Helical Device (LHD) was carried out in the 2nd experimental campaign[1],[2] in the end of 1998. During the experimental series, maximum 300kW/0.2sec of ICRF power was injected to the LHD plasma by using a pair of loop antennas. This paper reports the installation of antennas and the results of coupling and heating experiments.

Target plasma was produced by 2nd harmonic ECH heating of 84GHz gyrotrons at a magnetic field of 1.5 Tesla. Target plasma density was quite low of less than $1x10^{19}m^{-3}$. Therefore the maximum injected power was limited by low coupling resistance of plasma. The heating efficiency and heating species were changed by the minority ion gas-puffing rate. For the optimum condition of the minority ion ratio (H/He~0.3), the plasma internal energy was increased from 13kJ to 26kJ. The heating power of ECH and ICRF were about 300kW in each. The diamagnetic measurement showed that ICRF heating has good efficiency comparable to the ECH heating in this power range.

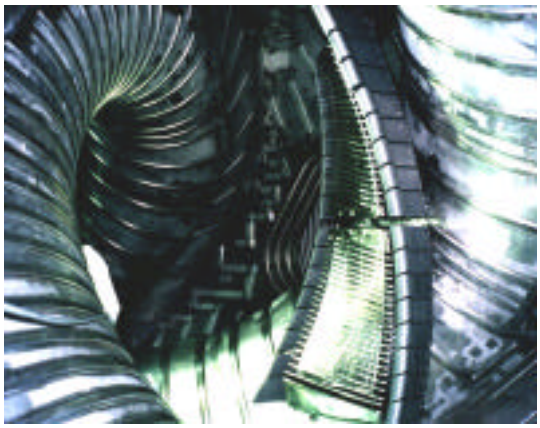

Fig.1 Photograph of ICRF loop antennas in LHD vacuum chamber

The position of the launcher section of the loop antenna can be changed. By changing the distance between the last closed flux surface (LCFS) and the launcher front from 9cm to 5cm, the antenna coupling resistance was almost doubled. In the ICRF heating experiment, the antenna front was usually placed at around 6cm from the last closed flux surface.

ANTENNA INSTALLATION AND PLASMA COUPLING

One pair of the loop antennas was inserted from the top and the bottom vertical ports of the LHD. These antennas are designed to launch the fast magnetosonic wave in the ion cyclotron range of frequency. Photograph of the loop antennas in the LHD vacuum chamber is shown

in Fig.1. The launcher section in the figure is divided to two separate parts. Upper section is fed through the top port and lower section is fed through the bottom port. The antenna launching section is just in front of the helical winding which is seen as ridged helical structures and is placed on the outboard side of toroid. The shape of the launcher is designed and fabricated to fit the plasma scrape off layer. The shape is 3 dimensional twisted form as shown in the figure. The total sizes of the antenna launching section are 120 cm in length (include upper and lower antenna), 46 cm in width and 17 cm in depth. Center current strap is one strap type, therefore the parallel wave number is not regulated. Usually antenna of one strap type from low field side excitation has an impurity problem in tokamaks. However in helical device as LHD, this antenna location is the high field side excitation even if antenna is located at the outboard side. Faraday shield is single layer and each pipe is directed to the external DC magnetic field.

The antennas have strong cooling channels for long pulse operation. The steady state technologies obtained in the R&D tests are fully incorporated in the design of the loop antenna [3]. The swing motion with the pivot point near the feedthrough section realizes position shift of the launcher section. The shift length is 15cm and elapsed time is around 10 sec. Throughout the experiment, the antenna position was changed to fit the experimental requests of the LHD.

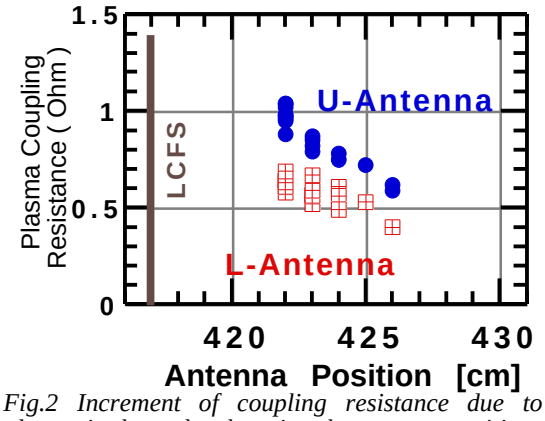

Fig.2 Increment of coupling resistance due to plasma is shown by changing the antenna positions (Faraday shield surface) between plasma last closed flux surface (LCFS) and vacuum vessel wall.

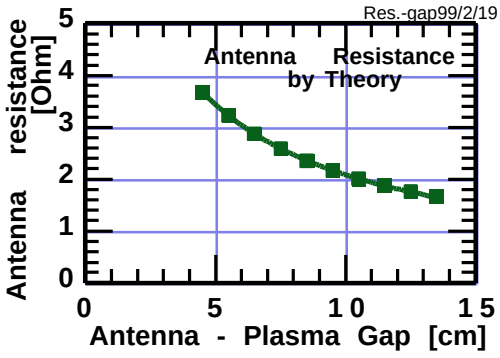

Fig.3 Calculation of antenna loading resistance by slab plasma model. Antenna structures of length, width, depth and shorted end are included in the model. Calculation parameters are same with in Fig.2.

Plasma coupling resistance was measured by changing the distance between the antenna and the plasma surface. In Fig.2, the coupling increments due to the plasma are shown. On the equatorial plane, last closed flux surface (LCFS) is at 417cm and vacuum vessel wall is at 451.5cm. Experimental conditions are as follows; B=1.5Tesla, ne-average=$8\times10^{19}m^{-3}$, H/(H+He)=0.3, frequency= 25.6MHz. In both antenna loops, coupling resistances were varied around twice by changing the positions. The vacuum loading level is almost half value of the nearest ones. Therefore the coupled power was 60-70% of the transmitter power. The coupling resistance values of two antenna loops were different. The reason of this difference is not clear. One of the candidates is the difference of antenna grounding structure. The lower antenna has three thin copper straps to ground the antenna back-plate to the vacuum vessel wall. One the other hand, there is no strap for grounding at the upper antenna.

The antenna resistance was calculated analytically to compare the experimental data. In Fig.3, theoretically calculated resistance was shown by changing the antenna positions. The model is two dimensional slab model and basic formulation is same with that of Reference [4]. The antenna current strap model includes length, width and shorted end and feeder section. And plasma is one dimensional slab structure. The range of the experimental condition in

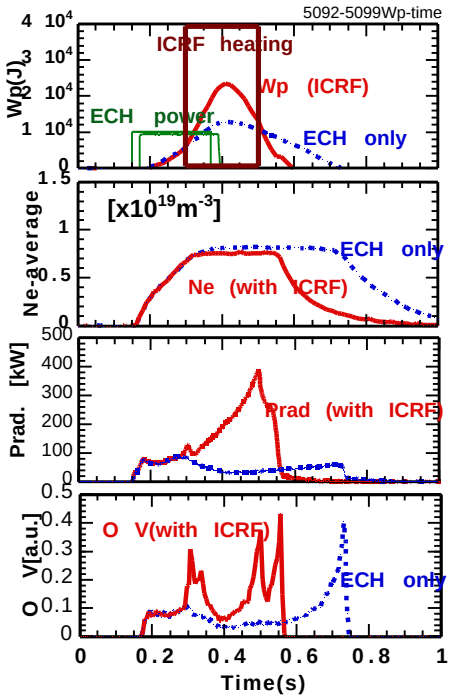

Fig.4 Time evolution of plasma parameters of ICRF heated plasma and target ECH plasma. (B=1.5Tesla, ne-average=8x10^{18}m^{-3}, H/(H+He)=0.3, Frequency = 25.6MHz)

Fig.2 is between from 7cm to 11cm on horizontal axis. The absolute value of the calculation is larger than the experimental value about factor two. It mainly depends on the boundary parameters on the calculation. But the decay curve is almost same with the experimental ones. This agreement suggests that the antenna coupling on the experiment was mainly due to the fast magnetosonic wave.

HEATING EXPERIMENTS

Heating experiment was carried out when the magnetic field of LHD was 1.5 Tesla and the RF frequency was 25.6 MHz. In this condition, the cyclotron layer and the mode conversion layer were located at the 0.5-0.7 of radius. Time evolutions of the plasma parameters are shown in Fig.4. The stored energy, line averaged electron density, impurity line (OV) and radiation power are shown. Dotted line is of the ECH target plasma and solid line is of the ICRF heated plasma. ICRF pulse was applied at 0.3 sec to 0.5sec and about one third of the duration was overlapped with the ECH pulse. Plasma energy was raised from 13kJ to 23.5kJ. During the ICRF operation, the plasma density is sustained at constant level.

Electron temperature profiles of target plasma and ICRF heated plasma are shown in Fig.5. In all radius, electron temperatures were increased. However the increasing rate in peripheral region was higher than in central region. The mode conversion region from the fast wave to the IBW was located at 0.65-0.8 radius and it agreed that the peripheral region was apparently heated. Radiation power and some impurity lines are increased during the ICRF pulse. The stored energy began to decrease during the ICRF pulse and this is consistent with the increase of the radiation power. Oxygen and iron impurity lines were increased during ICRF pulse. These increases depended on the minority ion ratio, which is directly related with the wave damping mechanism.

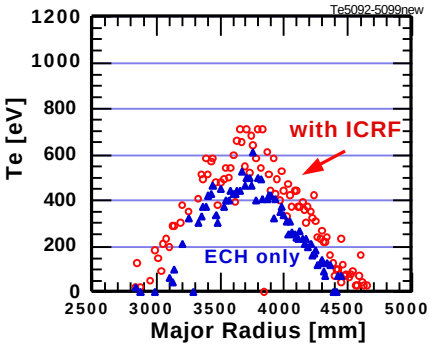

Fig.5 Electron temperature profiles of target ECH plasma and ICRF heated plasma at 0.38sec.of Fig.4.

Heating properties were largely affected by the minority ion ratio H/(H+He). In Fig.6, the increments of total stored energy Wp, and the incremental electron stored energy We, due to ICRF heating are shown by changing the minority ion ratio. This experiment was conducted by increasing the hydrogen gas-puff amount. On the other hand the majority helium gas was constant. Therefore the electron density was slightly increased as increasing the minority ion ratio. Wp is diamagnetic signal and electron stored energy We is calculated from the temperature of Thomson scattering and the density of FIR interferometer. To achieve the high Wp discharges, it was necessary to add the minority ion of over than 20 %. If the H ratio was less than 15%, no electron heating was observed. Wp-We seems to be the increment of ion component.

To understand the wave heating mechanism in the LHD, one dimensional wave analysis code [5] was used. This code includes the effects of the wave propagation, damping process,

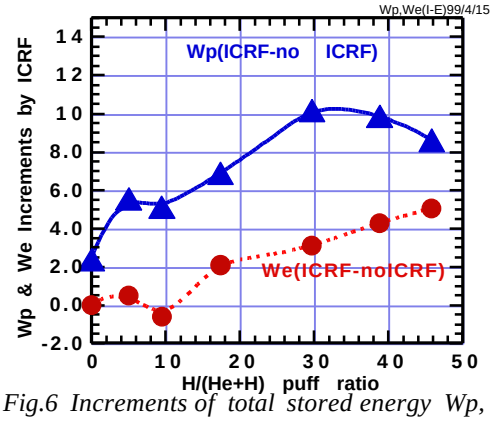

Fig.6 Increments of total stored energy Wp, and electron stored energy We versus input gas puff ratio H/(He+H). (Wp; diamagnetic loop, We ; Thomson Te(r) and FIR ne(r))

mode conversion, eigen mode formation in one dimension and current drive. Figure 7 shows the power partitions to plasma species from the launched wave. The calculation was done for the parameters along the line on the equatorial plane of LHD. On the low H ratio region, there is small electron heating and hydrogen cyclotron damping mainly is occurred. This is so-called minority heating region. On the medium H ratio region, there is electron heating by mode conversion. In the higher H ratio region, fast wave evanescent layer becomes thick, then excited fast wave is reflected at a left-hand cut-off. In this range, minority ion cyclotron damping is dominant.

The experimental results of Fig.6 agree qualitatively with this calculation. The gas puff ratio of H/(H+He) was not exactly appeared on plasma species. Due to the high recycling rate of helium particles, the proton ratio in plasma was seemed to be lower than the input gas puff ratio.

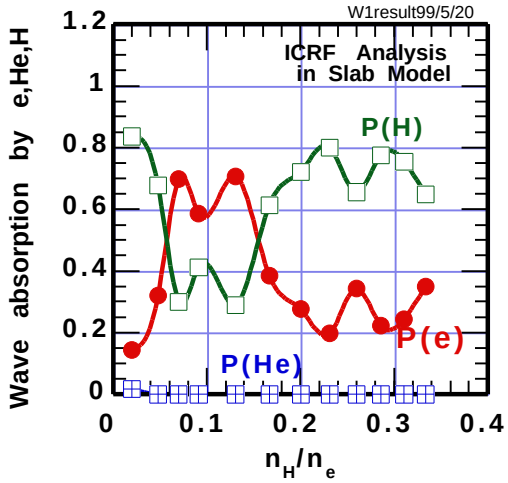

Fig.7 Wave absorption analysis on a slab plasma model shows that electron absorption is occurred at minority hydrogen content of 5 to 15 % of electron.

SUMMARY

Initial ICRF heating experiment in the LHD was carried out in 1998. One pair of the movable loop antennas was used and the coupling resistance was around one ohm for the low density ECH plasma. The loading characteristics were consistent with the fast wave excitation. By applying the ICRF heating of 300 kW to the ECH target plasma, the diamagnetic energy was increased from 13 kJ to 26 kJ. The heating performance was decided by hydrogen mixture rate on puffing gas. Efficient electron heating was observed at higher hydrogen gas ratio. These results can be explained by the one dimensional wave analysis calculation on slab plasma model. On the experiment of 1999, the magnetic field of the LHD will be increased to 2.8 Tesla and the RF frequency will be also raised. The higher frequency and higher density plasma should lead to the better plasma coupling and higher heating power. In addition, another new type antenna (Folded Wave-Guide antenna) is installed and will be operated in 1999.

REFERENCES:

[1] O. Motojima, et al., Physics of Plasmas, Vol.6,No5, (1999) 1843
[2] M. Fujiwara, et al., this conference
[3] T. Mutoh, et al., Journal of Plasma and Fusion Research, SERIES, Vol.1, (1998) 334
[4] K.Theilhaber, J.Jacquinot, Nuclear Fusion, Vol.24, (1984) 541
[5] A. Fukuyama, et al., Computer Physics Report 4 (1986) 137